

# Energy-based design base shear for RC frames considering global failure mechanism and reduced hysteretic behavior

Onur Merter<sup>\*1</sup> and Taner Ucar<sup>2a</sup>

<sup>1</sup>Department of Civil Engineering, Dokuz Eylul University, 35160, Buca, Izmir, Turkey

<sup>2</sup>Department of Architecture, Dokuz Eylul University, 35160, Buca, Izmir, Turkey

(Received June 24, 2016, Revised May 8, 2017, Accepted May 13, 2017)

**Abstract.** A nonlinear static procedure considering work-energy principle and global failure mechanism to estimate base shears of reinforced concrete (RC) frame-type structures is presented. The relative energy equation comprising of elastic vibrational energy, plastic strain energy and seismic input energy is obtained. The input energy is modified with a factor depending on damping ratio and ductility, and the energy that contributes to damage is obtained. The plastic energy is decreased with a factor to consider the reduced hysteretic behavior of RC members. Given the pre-selected failure mechanism, the modified energy balance equality is written using various approximations for modification factors of input energy and plastic energy in scientific literature. External work done by the design lateral forces distributed to story levels in accordance with Turkish Seismic Design Code is calculated considering the target plastic drift. Equating the plastic energy obtained from energy balance to external work done by the equivalent inertia forces considering, a total of 16 energy-based base shears for each frame are derived considering different combinations of modification factors. Ductility related parameters of modification factors are determined from pushover analysis. Relative input energy of multi degree of freedom (MDOF) system is approximated by using the modal-energy-decomposition approach. Energy-based design base shears are compared with those obtained from nonlinear time history (NLTH) analysis using recorded accelerograms. It is found that some of the energy-based base shears are in reasonable agreement with the mean base shear obtained from NLTH analysis.

**Keywords:** failure mechanism; structural damping; seismic input energy; hysteretic properties; modification factors; energy-based base shears

## 1. Introduction

Earthquakes may cause several damages to buildings depending upon different geophysical and structural factors. The magnitude, intensity and duration of earthquake, type of soil or fault properties are important parameters that may affect the structural damage. However, poorly designed and constructed non-engineered structures are probably the most vulnerable structures exposed to earthquake hazard. Although there may exist moderate, heavy or major damages under seismic effects, the crucial aspect of structural engineering is to prevent the total collapse of structures. Therefore, when new structures are designed, the failure mechanism of structures under earthquake effects should be considered as to prevent unreasonable failure modes, such as soft-story or local failure mechanisms. Designing structures in accordance with an admissible global failure mechanism, where inelastic flexural deformations are assumed to concentrated in plastic hinge regions at both ends of all beams and base columns, could provide nearly uniform drift over the height of the structure and an admirable structural energy dissipation capacity

related with high level of ductility. In order to control the failure mechanism, seismic capacity of structural systems may be enhanced and the whole structure is desired to design stable.

A critical matter of seismic assessment of structures is the proper determination of inelastic deformation mechanisms (Priestley 1996). Potential inelastic deformation regions of structures may be associated with failure mechanisms which have generally two types as local and global (Zhe and Lieping 2009). Local story mechanisms have vulnerable failure profiles and may cause to undesired progressive collapse. The preferable collapse mode under seismic effects is generally global failure mechanism with strong columns and weak beams to prevent total collapse (El Ezz 2008). However, structures which are seismically designed may certainly not have strong column-weak beam failure mechanism (Bai and Ou 2012). Severe ground motions can cause undesirable failure mechanisms on structures which behave nonlinear under seismic actions. To this respect, it may be a rational aspect to design new structures against earthquake effects ensuring the strong column-weak beam failure mechanism (Leelataviwat and Goel 2002, Liao 2010, Bai and Ou 2012).

Earthquake resistant structural design procedures in current seismic design codes are traditionally strength based and less commonly direct displacement based (Priestley *et al.* 2007, Muljati *et al.* 2015). The strength and displacement capacity of structural members are not desired

\*Corresponding author, Ph.D.

E-mail: [onur.merter@deu.edu.tr](mailto:onur.merter@deu.edu.tr)

<sup>a</sup>Assistant Professor

E-mail: [taner.ucar@deu.edu.tr](mailto:taner.ucar@deu.edu.tr)

to be less than seismic demands of earthquakes in these procedures. Displacement-based procedures became more important especially in the 21<sup>st</sup> century than strength based methods, where elastic earthquake forces are reduced by adopting an arbitrary force reduction factor in order to account for the potential inelastic response associated with the material and the structural system. Related to displacement-based procedures, performance-based design philosophy has recently become popular because of the estimation of structural vulnerability depending upon the nonlinear displacements of structures (Calvi *et al.* 2008). Additionally, for structures which are generally expected to behave nonlinear under seismic actions, energy-based design approaches provide an alternative among the other methods (Akbaş and Shen 2003, Dogru *et al.* 2015). Structural stability in energy-based design and assessment is thought as the balance between the energy demand and energy absorption capacity of the structure. Earthquake ground motion may be interpreted as energy input to the structure and thus more rational seismic approach is considered (Leetaviwat *et al.* 2009, Lopez-Almansa *et al.* 2013). In literature, many researchers made innovative studies about the energy concept in seismic design and the use of energy in earthquake resistant structural design (Housner 1956, Akiyama 1985, Uang and Bertero 1990). Energy balance concept for structures under seismic effects was widely used in the design and performance-based plastic design procedure was proposed to evaluate structures from the viewpoint of nonlinear behavior (Chao and Goel 2005, Leetaviwat *et al.* 2008, 2009, Bayat *et al.* 2008, Liao 2010, Massumi and Monavari 2013, Paolacci 2013).

Design of hysteretic model parameters directly affects the nonlinear response of structures. Hysteretic behavior of structural systems has an important influence on determination of nonlinear energy capacity of structures (Bai and Ou 2012, Kazantzi and Vamvatsikos 2012, Kim 2012). Strength and stiffness degradation and pinching effects in hysteresis loops of ductile RC structural systems under seismic excitations are crucial for accurately estimating the energy dissipation capacity. Therefore, hysteretic properties of structural systems should be properly characterized in precise energy-based design and assessments. Various hysteretic models, which characterize the nonlinear hysteretic properties of structural components under cyclic load reversals, are available for use in nonlinear structural analyses (FEMA P440A 2009). These are analytical models (hysteresis rules) which are set up considering the experimental tests of structural members and they range from simple elasto-plastic model to complex strength and stiffness degrading curvilinear hysteretic models.

Global failure mechanism considering strong column weak-beam principle is assumed in order to derive energy-based seismic design base shear force for multistory RC frames. The modified energy balance equation is written considering the reduced hysteretic behavior. Input energy is modified with a factor due to damping effects, and the energy that contributes to damage is obtained. Relative earthquake input energy of equivalent single degree of

freedom (SDOF) system is calculated considering the elastic velocity response spectra and converted to MDOF  $n$ th mode input energy contribution using the modal-energy-decomposition approach. The energy-based design base shear force is obtained from work-energy principle equating the plastic energy of MDOF system to the external work done by the equivalent inertia forces. Considering various modification factors of plastic energy (Gulkan and Sozen 1974, Kowalsky 1994, Priestley 2003, Dwairi *et al.* 2007) and input energy (Akiyama 1985, Kuwamura and Galambos 1989, Fajfar and Vidic 1994, Benavent-Climent *et al.* 2002, Benavent-Climent *et al.* 2010) existed in scientific literature, different base shear forces are obtained. Energy-based design base shears are compared with those values obtained from NLTH analysis of several RC frames using real ground motion records. Thereby, the validation of different approaches on plastic energy modification factor related to hysteretic damping and seismic input energy modification factor is investigated.

## 2. Global failure mechanism

Energy calculations in nonlinear behavior of the structures are directly related to the number of plastic sections, i.e., proper modelling of inelastic deformations has an importance from the viewpoint of plastic energy calculations of MDOF structural systems. There are some hypotheses about modelling of inelastic behavior of structural components. Typically, the use of a lumped plasticity approach based on conventional plastic hinge hypothesis may be convenient for many structural engineering practices (Kappos *et al.* 2012). Plastic hinge hypothesis provides the advantage of relatively modest computational afford when compared with the distributed plasticity approach based on fiber analysis. Plastic hinges inevitably form at the end of frame members where maximum moments are expected to develop under lateral loads.

Failure (or yield) mechanisms are indicators of robustness and functionality level of structures under seismic effects. Frame structures may have many failure mechanisms such as local failure mechanism, soft-story mechanism and global failure mechanism (Bai and Ou 2012). Plastic hinges form at the ends of columns of the stories in local or soft-story failure mechanism and hence

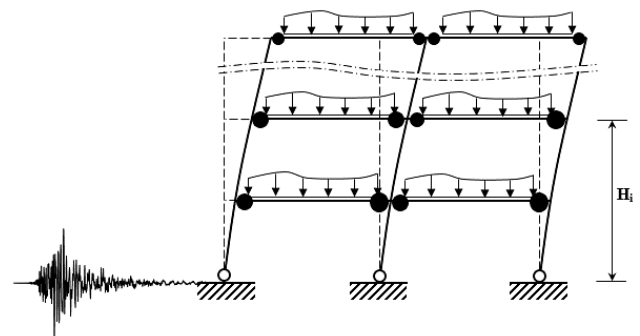


Fig. 1 Ideal (global) failure mechanism of a MDOF system

the stability of vertical members under gravity loads may not be preserved causing a catastrophic collapse. Accordingly, flexural plastic deformations concentrate first at beam ends, then at the base of first story columns in global failure mechanism. Total collapse is prevented by satisfying strong column-weak beam design principle, which leads to a ductile collapse (Fig. 1). Ideal (global) failure mechanism is designated for energy-based computations of the study and derivation of seismic design base shear force controlling the yield mechanism of the structure is therefore preliminarily aimed.

### 3. Energy response parameters and energy balance concept

Energy is a dynamic based concept in structural and earthquake engineering and the dynamic equation of motion of structural systems should be extendedly analyzed because of this reason. Like many other fundamental parameters of structural dynamics, energy related concepts are first formulated based on SDOF system. The general differential equation of motion of an inelastic lumped-mass SDOF system subjected to a ground motion is (Chopra 1995)

$$m \cdot \ddot{u} + c \cdot \dot{u} + f_s(u) = -m \cdot \ddot{u}_g(t) \quad (1)$$

where  $u$  is the relative displacement of a SDOF system,  $m$  is the mass,  $c$  is the damping coefficient,  $f_s(u)$  is the resisting force for nonlinear system and  $u_g(t)$  is the ground displacement. The energy balance equation of a SDOF system subjected to a ground motion may be expressed by integrating the equation of motion with respect to displacement (classical work-energy principle). Multiplying both sides of Eq. (1) by  $du = \dot{u} dt$  and integrating along the entire duration of earthquake ( $t_0$ ) give the energy balance equation of a fixed-based SDOF system

$$\int_0^{t_0} m \cdot \ddot{u} \cdot \dot{u} dt + \int_0^{t_0} c \cdot \dot{u}^2 dt + \int_0^{t_0} f_s(u) \cdot \dot{u} dt = \int_0^{t_0} -m \cdot \ddot{u}_g(t) \cdot \dot{u} dt \quad (2)$$

The first term on the left side of Eq. (2) indicates the relative kinetic energy ( $E_K$ ), the second term indicates the energy dissipated by the inherent damping ( $E_\xi$ ) and the third term indicates the energy absorbed by the spring ( $E_S$ ). The right term of the equation shows, by definition, the relative earthquake input energy ( $E_I$ ). The relative energy equation of SDOF system is then expressed as

$$E_K + E_\xi + E_S = E_I \quad (3)$$

If the expansion of the energy of the resisting force is written, Eq. (4) is obtained

$$E_K + E_\xi + [E_{Se} + E_p] = E_I \quad (4)$$

where  $E_{Se}$  is the recoverable elastic strain energy component and  $E_p$  is the irrecoverable hysteretic energy (the plastic strain energy) component of the energy of the resisting force. The sum of these energies gives the total absorbed

energy by the nonlinear spring. In Eq. (4), the sum of ( $E_K + E_{Se}$ ) constitutes the total elastic vibrational energy ( $E_e$ ) of the system. So that Eq. (4) can be rewritten as (Akiyama 1985, Bai and Ou 2012)

$$E_e + E_\xi + E_p = E_I \quad (5)$$

The energy equation can be expressed in the following form by taking the energy component dissipated by the inherent damping ( $E_\xi$ ) to the right side of Eq. (5)

$$E_e + E_p = E_I - E_\xi \quad (6)$$

The left hand side of Eq. (6) comprises only the elastic vibrational ( $E_e$ ) and plastic energy ( $E_p$ ) components and the difference between  $E_I$  and  $E_\xi$  on the right hand side indicates the energy input contributable to damage of the structure ( $E_D$ ) (Housner 1956, Bai and Ou 2012, Lopez-Almansa *et al.* 2013). The energy  $E_D$  is the multiplication of input energy ( $E_I$ ) with a factor  $\lambda$ , which depends on the damping ratio ( $\xi$ ), ductility ( $\mu$ ) and the cumulative ductility factor ( $\eta$ ) (Akiyama 1985, Kuwamura and Galambos 1989, Fajfar and Vidic 1994, Benavent-Climent *et al.* 2002, Benavent-Climent *et al.* 2010). In Eq. (7),  $\lambda$  is the modification factor of earthquake energy input due to the damping (Bai and Ou 2012)

$$E_e + E_p = E_D = \lambda \cdot E_I \quad (7)$$

The plastic energy ( $E_p$ ), the energy dissipated by the damping ( $E_\xi$ ) and the total elastic vibrational energy ( $E_e$ ) of a SDOF system subjected to a ground motion can be determined from NLTH analysis and energy-time variation graph of a structure may be obtained as shown in Fig. 2.

The energy dissipation capacity of RC members under cyclic loading decreases due to combined stiffness and strength degradation and pinching effects, which are particularly common in RC members. The area enclosed by the hysteresis loops of hysteretic model with moderate or severe pinching behavior is smaller than the area of the hysteresis loops of elasto-plastic or strength hardening non-degrading piecewise linear hysteretic models, which have stable hysteresis loops. Also, if a structural member exhibits some level of stiffness degradation or experiences a strength degradation due to increasing inelastic displacements or repeated cyclic load reversals, the area enclosed by the hysteresis loops will decrease. Therefore; reduced hysteretic behavior of structural members should be considered while

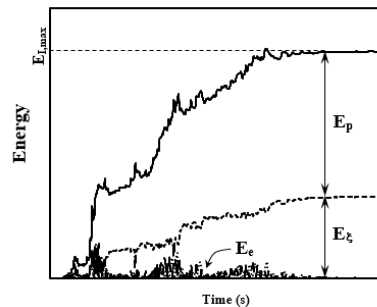


Fig. 2 Energy time history of a nonlinear SDOF system

the energy dissipation of structures is computed and the hysteretic (or plastic) energy of the system for the stable models (generally elasto-plastic or bilinear strength hysteretic model) should be modified with a factor to consider the reduced hysteresis rules (Bai and Ou 2012). For these reasons, the plastic energy can be modified with a factor  $\eta_p$ . Otherwise, calculation of irrecoverable hysteretic energy based on stable hysteresis loops will overestimate the energy dissipation capacity resulting in excessive damage. The energy equation, which is acceptable for all structural systems, is rewritten by using the factor  $\eta_p$  as

$$E_e + \eta_p \cdot E_p = \lambda \cdot E_I \quad (8)$$

### 3.1 Plastic energy modification factor ( $\eta_p$ )

Derivation of seismic design base shear force within this study considers the energy approach and global failure mechanism of multistory RC frame structures. The work needed to push structures to the target drift is assumed to be equal to the energy dissipated in plastic hinges of the global failure mechanism (Leelataviwat and Goel 2002, Liao 2010, Bai and Ou 2012). Hysteretic behavior of plastic hinges, which have direct influence on energy dissipation capacity, is essential for accurate estimation of energy-based base shears. However, hysteretic behavior of RC members is not stable and smooth and the reduction in the area of hysteresis loops is required (Bai and Ou 2012). Fig. 3 shows the smooth and the reduced hysteresis loops together, where  $A_F$  is the area of full hysteresis loop and  $A_P$  is the area of hysteresis loop with strength degradation and pinching effects.  $\Delta_y$  and  $\Delta_{max}$  are the yield and the maximum displacements, respectively and  $K_i$  and  $K_{eff}$  are the elastic and the effective stiffnesses, respectively. The  $r$  indicates the post-yield stiffness or the second-slope stiffness ratio and  $rK_i$  is the slope (secondary stiffness) of the hysteresis loop. R-P-P is the rigid-perfectly-plastic hysteresis loop as mentioned in Jacobsen's approach to obtain the equivalent damping value (Jacobsen 1930, Dwairi 2004). The modification factor of plastic energy ( $\eta_p$ ) is given by (Bai and Ou 2012)

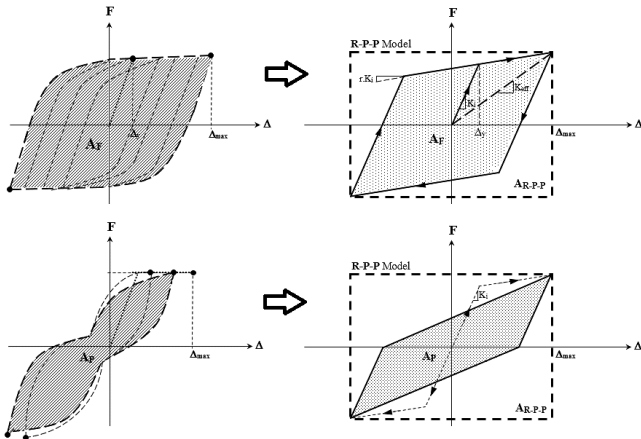


Fig. 3 Smooth and reduced (pinched) hysteresis models

$$\eta_p = \frac{A_p}{A_F} = \frac{A_{RPP}}{A_F} \cdot \frac{A_p}{A_{RPP}} = \left[ \frac{\mu \cdot (1+r \cdot \mu - r)}{(\mu-1) \cdot (1-r)} \right] \cdot \frac{A_p}{A_{RPP}} \quad (9)$$

where  $\mu = \Delta_{max}/\Delta_y$  is the ductility ratio. The ratio of  $A_{RPP}/A_F$  in Eq. (9) can be obtained from geometry by using the rectangular area of R-P-P model and the trapezoid area of bilinear model (Fig. 3). To find out the ratio of  $A_p/A_{RPP}$ , the concept of equivalent viscous damping corresponding to the hysteretic response should be researched. This value depends on the displacement ductility and the location of plastic hinges in the elements. Equivalent viscous damping ( $\xi_{eq}$ ) is generally interpreted as the superposition of initial elastic ( $\xi_0$ ) and hysteretic ( $\xi_H$ ) damping components as

$$\xi_{eq} = \xi_0 + \xi_H \quad (10)$$

Elastic damping component ( $\xi_0$ ) is widely accepted as 5% for typical RC structures. However, hysteretic damping that represents the dissipation due to nonlinear hysteretic behavior depends essentially on the post-yielding characteristics of the element. Jacobsen (1930) defined the hysteretic damping ratio by using the energy dissipated in harmonic vibration. By integrating the second energy term of Eq. (2) from  $t_0=0$  to  $t_0=2\pi/\omega$ , the energy dissipated by viscous damping ( $E_\xi$ ) in one cycle of harmonic vibration may be obtained as (Chopra 1995)

$$E_\xi = \pi \cdot c \cdot \omega \cdot u_0^2 = 2 \cdot \pi \cdot \xi \cdot \frac{\omega}{\omega_n} \cdot k \cdot u_0^2 \quad (11)$$

where  $c$  is the damping coefficient,  $\omega$  is the natural frequency of harmonic loading,  $k$  is the stiffness and  $u_0$  is the displacement amplitude. Damping for a perfectly symmetric hysteretic cycle in harmonic loading can be seen in Fig. 4, where  $E_{dis}$  is the energy dissipated by the system and  $E_{sto}$  is the elastic strain energy stored by the system ( $E_{sto} = k \cdot u_0^2 / 2$ ).

With reference to Fig. 4, the equivalent viscous damping can be obtained by equating the energy dissipated in viscous damping given by Eq. (11) to the energy dissipated in the structure ( $E_{dis}$  in Fig. 4). Assuming the resonance condition ( $\omega_n = \omega$ ), the final result of hysteretic damping ( $\xi_H$ ) is obtained as (Blandon 2004)

$$\xi_H = \frac{1}{4\pi} \cdot \frac{E_{dis}}{E_{sto}} \quad (12)$$

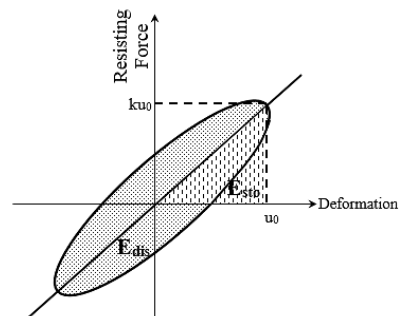


Fig. 4 Damping for a hysteretic cycle in harmonic loading

It is clear that the response of the real earthquake excitation cannot be exactly represented by steady-state harmonic response and the shape of hysteresis loop will not be exactly an ellipse. Consequently, there are some empirical proposals in literature for equivalent damping in RC elements under uniaxial loadings (Priestley *et al.* 2007, Dwairi *et al.* 2007, Rodrigues *et al.* 2012). For the theoretical R-P-P loop, which dissipates more energy than any other model, the hysteretic damping value of  $2/\pi$  is found by using Jacobsen's approximation. If stiffness and strength degradation and pinching effects are considered, the hysteretic damping is rewritten as a function of  $A_p/A_{RPP}$  ratio

$$\xi_H = \frac{2}{\pi} \cdot \frac{A_p}{A_{RPP}} \quad (13)$$

The Jacobsen's equation above is the simplest approach to estimate the hysteretic damping (Khan *et al.* 2016). Utilizing  $A_p/A_{RPP}$  ratio of Eq. (13) in Eq. (9), leads to the following equation of plastic energy modification factor ( $\eta_p$ )

$$\eta_p = \frac{\pi \cdot \mu \cdot (1+r \cdot \mu - r)}{2 \cdot (\mu-1) \cdot (1-r)} \cdot \xi_H \quad (14)$$

Many approaches and formulas are available in literature for estimation of  $\xi_H$ . Gulkan and Sozen (1974), gives the formula for  $\xi_H$  considering Takeda hysteretic model (Fig. 5) as

$$\xi_H = 0.2 \cdot \left( 1 - \frac{1}{\sqrt{\mu}} \right) \quad (15)$$

Kowalsky (1994) estimated  $\xi_H$  considering Takeda model with unloading and reloading stiffness factors  $\alpha$  and  $\beta$  of 0.5 and 0.0, respectively, as

$$\xi_H = \frac{1}{\pi} \cdot \left[ 1 - \frac{1-r}{\sqrt{\mu}} - r \cdot \sqrt{\mu} \right] \quad (16)$$

Fat and thin Takeda models, which are generally fitted for RC beams (frames) and columns (walls), are shown in Fig. 5 (Priestley *et al.* 2007, Mergos and Beyer 2014). For concrete frames, Priestley (2003) gives the  $\xi_H$  formula as

$$\xi_H = \frac{1.2}{\pi} \cdot \left( 1 - \frac{1}{\sqrt{\mu}} \right) \quad (17)$$

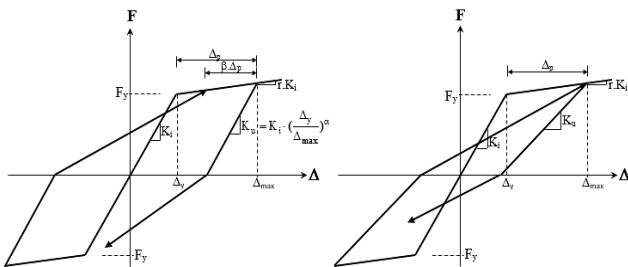


Fig. 5 Fat and thin Takeda hysteretic models

Dwairi *et al.* (2007) proposed Eq. (18) for  $\xi_H$  considering constant  $C$ , which depends on hysteresis rule and effective period. If  $T_{eff} \geq 1$  s then  $C=0.65$  and, if  $T_{eff} < 1$  s then  $C = 0.65 + 0.5 \cdot (1 - T_{eff})$

$$\xi_H = C \cdot \left( \frac{\mu-1}{\pi \cdot \mu} \right) \quad (18)$$

Eqs. (15)-(18) are considered for calculation of  $\xi_H$  in this study and substituting  $\xi_H$  into Eq. (14), the modification factor for plastic energy is computed. Fat (large) Takeda model is used for RC frame type structures.

### 3.2 Input energy modification factor ( $\lambda$ )

The difference between the input energy and the energy dissipated by the damping ( $E_I - E_\xi$ ) was first introduced by Housner (1956) as the energy input that contributes to structural damage ( $E_D$ ) (Lopez-Almansa *et al.* 2013). The energy  $E_D$  is given as

$$E_D = E_e + \eta_p \cdot E_p = \lambda \cdot E_I \quad (19)$$

where  $\lambda$  is the modification factor of input energy and can be written as the ratio of  $E_D/E_I$ . There are many empirical studies about the estimation of  $\lambda$  factor, however, in this study four of them are used. Akiyama (1985) defined the modification factor as a function of a structural damping as

$$\lambda = \frac{1}{(1 + 3 \cdot \xi + 1.2 \cdot \sqrt{\xi})^2} \quad (20)$$

Kuwamura and Galambos (1989) proposed the following equation

$$\lambda = \left( \frac{\frac{\eta}{\eta + 0.15}}{1 + \frac{20 \cdot (3 \cdot \xi + 1.2 \cdot \sqrt{\xi})}{\eta + 10}} \right)^2 \quad (21)$$

where  $\eta$  is the cumulative ductility ratio ( $\eta = E_H/F_y A_y$ ) (Lopez-Almansa *et al.* 2013). Depending on studies with elastic-perfectly-plastic (EPP) systems subjected to Friuli 1976, California 1979, Montenegro 1979, Banja Luka 1981 and Chile 1985 earthquakes, Fajfar and Vidic (1994) estimated  $\lambda$  for system with  $\zeta=0.05$

$$\lambda = 0.90 \cdot \frac{(\mu-1)^{0.95}}{\mu} \quad (22)$$

Modifying Akiyama's equation Benavent-Climent *et al.* (2002) proposed the following equation

$$\lambda = \left( \frac{1.15 \cdot \eta}{(0.75 + \eta) \cdot (1 + 3 \cdot \xi + 1.2 \cdot \sqrt{\xi})} \right)^2 \quad (23)$$

In this study,  $\lambda$  factor is calculated considering Eqs. (20)-(23) and then the energy balance is satisfied from Eq. (19). The graphical interpretation of elastic and plastic energies together with modification factors  $\eta_p$  and  $\lambda$  are shown in Fig. 6.

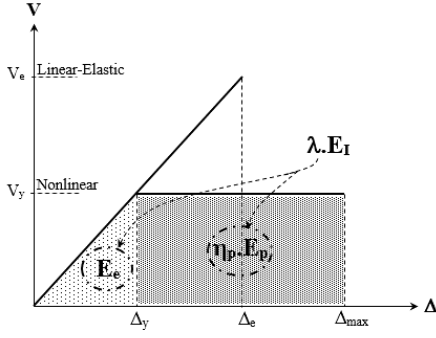


Fig. 6 Fundamental energy definitions

#### 4. Earthquake energy input ( $E_I$ ) to MDOF systems

In energy-based seismic analyses and assessments, the earthquake effect is considered as energy input to the structure. Earthquake input energy ( $E_I$ ) can be calculated from NLTH analyses. It is an important and main energy because of involving all other structural energy types, i.e., all other energy types like elastic and plastic energies arise from the input energy (Fig. 2). Based on Housner's assumption, the input energy of an equivalent  $n$ th mode SDOF system, a SDOF system with vibration properties of the  $n$ th mode of MDOF system, considering the elastic velocity response spectra ( $S_{V,n}$ ) can be approximated as

$$E_{I(SDOF)n} = \frac{1}{2} \cdot M_n \cdot S_{V,n}^2 = \frac{1}{8} \cdot \frac{M_n \cdot T_n^2}{\pi^2} \cdot S_{a,n}^2 \quad (24)$$

where  $M_n = \phi_n^T \cdot M \cdot \phi_n$  is the generalized mass and  $\phi_n$  is natural mode vector of the  $n$ th mode, respectively. If the pseudo-velocity ( $S_{V,n}$ ) is written in terms of pseudo-acceleration ( $S_{a,n}$ ) the equation consists of the natural period ( $T_n$ ) of the  $n$ th mode.

The equation of motion of a nonlinear MDOF system in terms of modal coordinates  $q_n(t)$  can be written as (Chopra 1995)

$$\ddot{q}_n(t) + 2 \cdot \zeta_n \cdot \omega_n \cdot \dot{q}_n(t) + \frac{f_n}{M_n} = -\Gamma_n \cdot \ddot{u}_g(t) \quad (25)$$

where  $\zeta_n$  is the damping,  $\omega_n$  is the natural frequency,  $f_n$  is the nonlinear restoring force vector,  $M_n$  is the generalized mass and  $\Gamma_n$  is the modal participation factor of the  $n$ th mode. Since Eq. (25) consists of a term  $\Gamma_n$ , the total absorbed energy for each mode of nonlinear MDOF systems may be expressed as (Uang and Bertero 1990, Chou and Uang 2003)

$$E_{absorbed,n} = \frac{1}{2} \cdot M_n \cdot (\Gamma_n \cdot S_{V,n})^2 \quad (26)$$

Relative earthquake input energy of equivalent SDOF systems can be calculated through NLTH analyses and converted to MDOF  $n$ th mode input energy contribution ( $E_{I(MDOF),n}$ ) as

$$E_{I(MDOF)n} = E_{I(SDOF)n} \cdot \Gamma_n^2 \quad (27)$$

The total earthquake input energy of MDOF system can

be estimated considering the summation of energies of the first few modes. Kalkan and Kunnath (2007) showed that taking three modes generally give very conservative results for MDOF systems while using the modal energy-decomposition approach. Therefore, considering the first three modes the total earthquake input energy of MDOF system may be approximated by using the modal energy-decomposition approach as (Bai and Ou 2012)

$$E_{I(MDOF)} = \sum_{n=1}^{N=3} E_{I(SDOF)n} \cdot \Gamma_n^2 \quad (28)$$

$$= E_{I(SDOF)1} \cdot \Gamma_1^2 + E_{I(SDOF)2} \cdot \Gamma_2^2 + E_{I(SDOF)3} \cdot \Gamma_3^2$$

Eq. (28) computes the total earthquake input energy of MDOF system considering the superposition of  $n$ th mode contribution. Since superposition principle does not apply in nonlinear systems, Eq. (28) seems to be arbitrary. However, this assumption constitutes the basis of studies related with relative input energy to MDOF system.

#### 5. Elastic energy ( $E_e$ )

Elastic vibrational energy comprises the relative kinetic energy and recoverable elastic strain energy. By comparison to other energy types, the elastic energy is not as significant as the others in nonlinear behavior. Elastic energy is far fewer than the plastic energy and the energy dissipated by damping mechanism (Fig. 2). Elastic vibrational energy is related with the linear-elastic part of Fig. 6 and Akiyama (1985) showed that it can be calculated with a reasonable accuracy as

$$E_e = \frac{1}{2} \cdot V_y \cdot \Delta_y = \frac{1}{2} \cdot M \cdot \left[ \frac{T_e}{2\pi} \cdot \frac{V_y}{W} \cdot g \right]^2 \quad (29)$$

where  $V_y$  and  $\Delta_y$  are yield (design) base shear and displacement, respectively,  $W$  is the total seismic mass,  $T_e$  is the elastic vibrational period and  $g$  is the acceleration of gravity.

#### 6. External work done by the system

The energy-based design base shear force ( $V_y$ ) may be distributed to story levels based on lateral load distributions of seismic design codes. In this study, the energy-based design base shear is calculated for the global failure mechanism of RC frames and is distributed to the story levels according to TSDC (2007). Accordingly, the work (plastic energy) done by design lateral forces is

$$E_p = \left( \sum_{i=1}^{N^{th} \text{ Story}} F_i \cdot H_i + \Delta F_N \cdot H_N \right) \cdot \theta_p \quad (30)$$

where  $F_i$  and  $H_i$  are the design lateral force and the height of the  $i$ th story, respectively,  $\Delta F_N$  is the additional equivalent seismic force acting on the top of the frame and  $H_N$  is  $N$ th story height (Fig. 7).  $\theta_p$  is the plastic design base rotation of

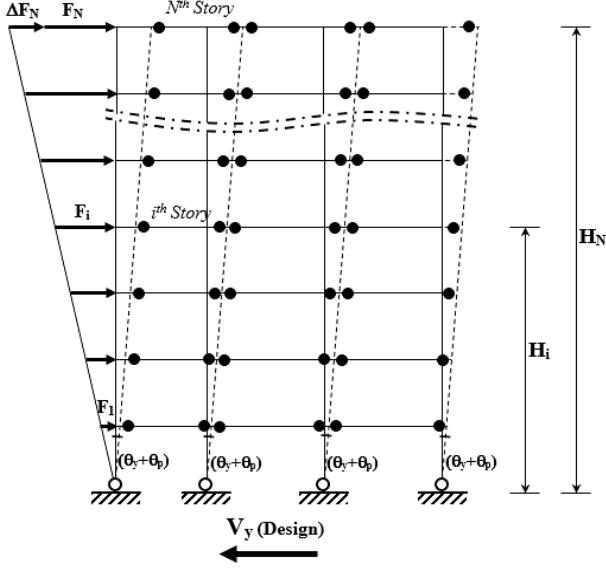


Fig. 7 Lateral design forces of a RC multi-story frame

the structure.

Assuming  $\Delta F_N = 0.0075 N V_y$  according to TSDC (2007) and  $\alpha_i \cdot V_y$  for  $F_i$  ( $F_i = \alpha_i \cdot V_y$  and  $\alpha_1 + \alpha_2 + \dots + \alpha_N = 1$ ), Eq. (30) is rewritten as (the classical work-energy principle)

$$E_p = V_y \cdot \theta_p \cdot \left[ \sum_{i=1}^{N^{\text{th}} \text{ Story}} \alpha_i \cdot H_i + 0.0075 \cdot N \cdot H_N \right] \quad (31)$$

where  $\alpha_i$  is the ratio of story forces to the total base shear force ( $F_i/V_y$ ).

## 7. Energy-based yield base shear force ( $V_y$ )

The energy-based yield base shear force is obtained from classical work-energy principle equating the plastic energy of MDOF system to the external work done by the equivalent inertia forces considering. First, the plastic energy equation is expressed in terms of  $\eta_p$  and  $\lambda$  factors, rearranging Eq. (19) and then is equated to Eq. (31)

$$\begin{aligned} & \frac{\lambda}{\eta_p} \cdot \sum_{n=1}^N E_{I(SDOF)_n} \cdot \Gamma_n^2 - \frac{1}{2} \cdot \frac{M}{\eta_p} \cdot \left[ \frac{T_e}{2\pi} \cdot \frac{V_y}{W} \cdot g \right]^2 \\ & = V_y \cdot \theta_p \cdot \left[ \sum_{i=1}^{N^{\text{th}} \text{ Story}} \alpha_i \cdot H_i + 0.0075 \cdot N \cdot H_N \right] \end{aligned} \quad (32)$$

The modification factors of plastic and earthquake input energy,  $\eta_p$  and  $\lambda$  in Eq. (32), are considered using Eq. (14) and Eqs. (20)-(23), respectively. The hysteretic damping ( $\zeta_H$ ) in Eq. (14) is calculated in accordance with Eqs. (15)-(18). For 4 different  $\eta_p$  and  $\lambda$  values, totally 16 different plastic energy equations are written. Energy-based yield base shear forces ( $V_y$ ) are summarized in Table 1. These forces are defined in terms of  $A$ ,  $B$ ,  $C^*$ ,  $D$ ,  $F$ ,  $G$ ,  $H$  and  $J$  coefficients which are obtained for 4 different values of  $\eta_p$  and  $\lambda$ . Table 1 indicates the modification factor matrix, too and  $V_y$  values are found considering these coefficients. For

example, if  $\eta_p$  is obtained from Eq. (14) using  $\zeta_H$  in Eq. (15) and  $\lambda$  from Eq. (20),  $V_y$  is calculated as  $-A + \sqrt{A^2 + B}$ . The coefficients of Table 1 are formulized and are expressed as in Eqs. (33)-(40)

$$A = \frac{0.4 \cdot W \cdot \pi^3 \cdot \sqrt{\mu} \cdot (1+r \cdot \mu - r) \cdot \left( \sum_{i=1}^{N^{\text{th}} \text{ Story}} \alpha_i \cdot H_i + 0.0075 \cdot N \cdot H_N \right) \cdot \theta_p}{T_e^2 \cdot g \cdot (\sqrt{\mu} + 1) \cdot (1-r)} \quad (33)$$

$$B = \frac{8 \cdot W \cdot \pi^2 \cdot \left( \sum_{n=1}^{N^{\text{th}} \text{ Mode}} E_{I(SDOF)_n} \cdot \Gamma_n^2 \right)}{T_e^2 \cdot g \cdot (1+3 \cdot \xi + 1.2 \cdot \sqrt{\xi})^2} \quad (34)$$

$$C^* = \frac{2 \cdot W \cdot \pi^2 \cdot \sqrt{\mu} \cdot (1+r \cdot \mu - r) \cdot (\sqrt{\mu} - r \cdot \mu + r - 1) \cdot \left( \sum_{i=1}^{N^{\text{th}} \text{ Story}} \alpha_i \cdot H_i + 0.0075 \cdot N \cdot H_N \right) \cdot \theta_p}{T_e^2 \cdot g \cdot (\mu - 1) \cdot (1-r)} \quad (35)$$

$$D = \frac{2.4 \cdot W \cdot \pi^2 \cdot \sqrt{\mu} \cdot (1+r \cdot \mu - r) \cdot \left( \sum_{i=1}^{N^{\text{th}} \text{ Story}} \alpha_i \cdot H_i + 0.0075 \cdot N \cdot H_N \right) \cdot \theta_p}{T_e^2 \cdot g \cdot (\sqrt{\mu} + 1) \cdot (1-r)} \quad (36)$$

$$F = \frac{2 \cdot C \cdot W \cdot \pi^2 \cdot (1+r \cdot \mu - r) \cdot \left( \sum_{i=1}^{N^{\text{th}} \text{ Story}} \alpha_i \cdot H_i + 0.0075 \cdot N \cdot H_N \right) \cdot \theta_p}{T_e^2 \cdot g \cdot (1-r)} \quad (37)$$

$$G = \frac{8 \cdot W \cdot \pi^2 \cdot \left( \sum_{n=1}^{N^{\text{th}} \text{ Mode}} E_{I(SDOF)_n} \cdot \Gamma_n^2 \right)}{T_e^2 \cdot g} \quad (38)$$

$$H = \frac{7.2 \cdot W \cdot \pi^2 \cdot \left( \sum_{n=1}^{N^{\text{th}} \text{ Mode}} E_{I(SDOF)_n} \cdot \Gamma_n^2 \right) \cdot (\mu - 1)^{0.95}}{T_e^2 \cdot g \cdot \mu} \cdot \left[ \frac{\eta \cdot (\eta + 10)}{(\eta + 0.15) \cdot (\eta + 10 + 60 \cdot \xi + 24 \cdot \sqrt{\xi})} \right]^2 \quad (39)$$

$$J = \frac{10.58 \cdot W \cdot \pi^2 \cdot \left( \sum_{n=1}^{N^{\text{th}} \text{ Mode}} E_{I(SDOF)_n} \cdot \Gamma_n^2 \right)}{T_e^2 \cdot g} \quad (40)$$

$$\left[ \frac{\eta}{(0.75 + \eta) \cdot (1 + 3 \cdot \xi + 1.2 \cdot \sqrt{\xi})} \right]^2$$

Selecting an appropriate post-yield stiffness ratio ( $r$ ) is

Table 1 Energy-based yield base shears in terms of coefficients A, B, C\*, D, F, G, H and J

		$\lambda$			
$\zeta_H$		Eq. (20)	Eq. (21)	Eq. (22)	Eq. (23)
$\eta_p$	Eq. (15)	$-A + \sqrt{A^2 + B}$	$-A + \sqrt{A^2 + G}$	$-A + \sqrt{A^2 + H}$	$-A + \sqrt{A^2 + J}$
	Eq. (16)	$-C^* + \sqrt{C^{*2} + B}$	$-C^* + \sqrt{C^{*2} + G}$	$-C^* + \sqrt{C^{*2} + H}$	$-C^* + \sqrt{C^{*2} + J}$
	Eq. (17)	$-D + \sqrt{D^2 + B}$	$-D + \sqrt{D^2 + G}$	$-D + \sqrt{D^2 + H}$	$-D + \sqrt{D^2 + J}$
	Eq. (18)	$-F + \sqrt{F^2 + B}$	$-F + \sqrt{F^2 + G}$	$-F + \sqrt{F^2 + H}$	$-F + \sqrt{F^2 + J}$

an important issue in nonlinear modeling (Ye *et al.* 2008). For short-period systems, sufficient post-yield stiffness may significantly reduce the maximum displacement whereas for mid- and long-period systems it may slightly increase the maximum displacement. However generally, the decreasing of post-yield stiffness ratio may increase the maximum displacement of the structure (Ye *et al.* 2008). Sufficient post-yield stiffness ratios should be selected to control the seismic performance of the structure. The ways to regulate the post-yield stiffness ratio may be defining the hardening features of the reinforcement and designing the structural geometry of the elements precisely. Higher values of the ratio  $r$  are not appropriate for damage assessment (Pampanin *et al.* 2002, Yazgan 2010, Greco 2014). 10% post-yield stiffness ratio is assumed in this study.

The plastic base rotation (design plastic drift ratio) ( $\theta_p$ ) is calculated as  $\theta_u - \theta_y$ , where  $\theta_u$  is the total rotation angle of the yield mechanism and  $\theta_y$  is the yield drift ratio (Fig. 7). Although there are some formulations in literature for  $\theta_y$  value of structures (Priestley *et al.* 2007), more accurate results can be obtained from nonlinear analysis. For seismic zones there are mapped probability levels of exceedance as 2%, 5% or 10%. These probability levels of exceedance are useful concepts in earthquake engineering when seismic hazard maps are created. For the probability level of exceedance 10% in fifty years period (the design earthquake), the maximum story drift ratio ( $\theta_u$ ) is suggested as 2% (Bayat *et al.* 2008, Liao 2010). The design earthquake of TSDC (2007) corresponds to this probability and  $\theta_u = 0.02$  is considered within the study.

## 8. Case study

Three-, ten- and seven-story RC frames with three, four and five bays, respectively, are considered as a case study. Frame-type structures are abbreviated as RCF\_3.3, RCF\_10.4 and RCF\_7.5 according to total story ( $N$ ) and bay number. Material strengths are assumed as 25 MPa for concrete and 420 MPa for longitudinal and transverse reinforcement steel. The total number of stories, beam spans, story heights ( $H_i$ ), and column and beam dimensions ( $b_c/h_c$  and  $b_{bi}/h_{bi}$ ) are presented in Table 2. Rectangular beams and square columns are considered in RC design. Typical view of frames with concentrated masses is shown in Fig. 8.

The values of uniformly distributed dead and live loads of RC beams ( $G_i$ ;  $Q_i$ ) and concentrated dead and live loads

of RC columns of typical stories ( $P_{Gi}$ ;  $Q_{Gi}$ ) and top stories ( $P_{GN}$ ;  $Q_{GN}$ ) are given Table 3. Frames are assumed to be located in seismic zone 1 and on Z3 soil group according to TSDC (2007). RC design of frames is performed using the structural analysis program SAP2000 (2016) and considering the requirements of TS500 (2000) and TSDC (2007). Concentrated seismic masses consisted of dead loads plus 30% of live loads are 223.78 tons, 1658.22 tons and 1185.24 tons for RCF\_3.3, RCF\_10.4 and RCF\_7.5, respectively. Eigenvalue analysis yields the natural vibration periods as 0.46 s, 1.02 s and 0.69 s for RCF\_3.3, RCF\_10.4 and RCF\_7.5, respectively.

Column longitudinal reinforcements of RCF\_3.3 are 8 $\phi$ 18 and 8 $\phi$ 16 for the first and other stories, respectively. 16 $\phi$ 24 and 16 $\phi$ 20 are provided in the column sections of RCF\_10.4 for the first and other stories, respectively, while column longitudinal reinforcement of RCF\_7.5 is 12 $\phi$ 20 for all stories. Longitudinal reinforcements in beams of RCF\_3.3 for the first and second stories are 6 $\phi$ 16 at the top and 3 $\phi$ 16 at the bottom. In the third story of RCF\_3.3, beam reinforcements are 4 $\phi$ 14 at the top and 3 $\phi$ 14 at the bottom. Beam reinforcements of RCF\_10.4 between the stories of 1 and 5 are 9 $\phi$ 18 at the top and 6 $\phi$ 18 at the bottom. In other stories of RCF\_10.4, longitudinal reinforcements of beams

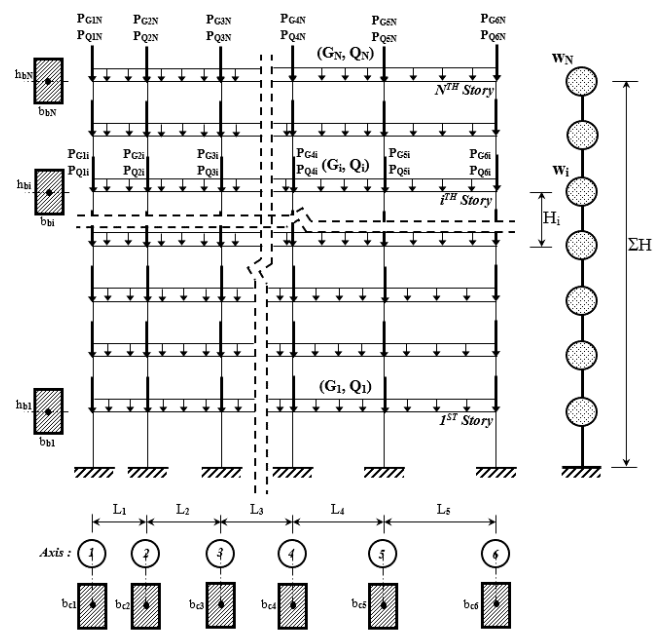


Fig. 8 Typical view of frames with vertical loads

Table 2 Geometrical properties of frame-type structures

# RC Frame	N	Beam Spans (m)	H <sub>i</sub> (m)	Column Dimensions (cm)	Beam Dimensions(cm)
RCF_3.3	3	L <sub>1,2&amp;3</sub> : 5.00	3.00	b <sub>c1-4</sub> : 40 h <sub>c1-4</sub> : 40 (All stories)	b <sub>bi</sub> : 25 h <sub>bi</sub> : 50 (All spans & stories)
RCF_10.4	10	L <sub>1</sub> : 4.00 L <sub>2</sub> : 5.30 L <sub>3</sub> : 5.30 L <sub>4</sub> : 4.00	3.00	b <sub>c1</sub> : 80 (70) h <sub>c1</sub> : 80 (70) b <sub>c2</sub> : 80 (70) h <sub>c2</sub> : 80 (70) b <sub>c3</sub> : 80 (70) h <sub>c3</sub> : 80 (70) b <sub>c4</sub> : 80 (70) h <sub>c4</sub> : 80 (70) b <sub>c5</sub> : 80 (70) h <sub>c5</sub> : 80 (70) 1 <sup>st</sup> story (Other stories)	b <sub>bi</sub> : 30 h <sub>bi</sub> : 60 (All spans & stories)
RCF_7.5	7	L <sub>1</sub> : 3.00 L <sub>2</sub> : 4.00 L <sub>3</sub> : 4.00 L <sub>4</sub> : 5.00 L <sub>5</sub> : 6.00	3.00	b <sub>c1</sub> : 60 h <sub>c1</sub> : 60 b <sub>c2</sub> : 60 h <sub>c2</sub> : 60 b <sub>c3</sub> : 60 h <sub>c3</sub> : 60 b <sub>c4</sub> : 60 h <sub>c4</sub> : 60 b <sub>c5</sub> : 60 h <sub>c5</sub> : 60 b <sub>c6</sub> : 60 h <sub>c6</sub> : 60 (All stories)	b <sub>bi</sub> : 30 h <sub>bi</sub> : 60 (All spans & stories)

are 7φ18 at the top and 5φ18 at the bottom. In the last two stories, 4φ18 and 3φ16 at the top and bottom of beams are provided. For beams of RCF\_7.5 between the stories 1-6, there are 5φ18 top reinforcements and 3φ18 bottom reinforcements. In the last story, 4φ18 at the top and 3φ16 at the bottom are provided.

### 8.1 Selection and scaling procedure of ground motion records

A total of seven recorded accelerograms are assembled according to the magnitude, distance, fault type, and soil profile type information. The accelerograms with a magnitude range of  $6.5 \leq M_w \leq 7.5$  and source-to-site distances ( $R_{JB}$ ) less than 100 km are compiled from the PEER-NGA strong-motion database, which is used as the main source (PEER, 2016). Since all frames are assumed to be located on site class Z3, the soil conditions of the accelerograms depict features of Z3 site class. A soil profile type definition of Z3 is considered as the counterpart of

NEHRP D site class, which is classified as  $180 \leq V_{S30} \leq 360$  m/s. The selected ground motions have strike-slip fault mechanism and effects of near fault are not considered. The list of ground motion records and the overall characteristics of accelerograms are presented in Table 4, where  $M_w$  is the moment magnitude of earthquake,  $R_{JB}$  is the Joyner-Boore distance,  $V_{S30}$  is the average of shear wave velocity in the first 30 m of the soil,  $PGA$  is the peak ground acceleration,  $PGV$  is the peak ground velocity and  $PGD$  is the peak ground displacement.

The selected ground motion records are scaled in terms of amplitude in time domain to make them compatible with the code-specific hazard level, which is generally defined in the form of an elastic response spectrum of acceleration. The scaling procedure used herein is based on minimizing the differences between the scaled response spectrum and horizontal elastic design spectrum of TSDC for local site class Z3 by using the method of least-squares. This way, a total of seven scaled accelerograms fulfilling duration and amplitude related requirements of TSDC for NLTH analysis

Table 3 Dead and live loads of beams and columns

#RC Frame	$G_i; Q_i$ (kN/m)	$G_N; Q_N$ (kN/m)	$P_{G1i}$	$P_{G2i}$	$P_{G3i}$	$P_{G4i}$	$P_{G5i}$	$P_{G6i}$
			$P_{Q1i}$	$P_{Q2i}$	$P_{Q3i}$	$P_{Q4i}$	$P_{Q5i}$	$P_{Q6i}$
			$P_{G1N}$	$P_{G2N}$	$P_{G3N}$	$P_{G4N}$	$P_{G5N}$	$P_{G6N}$
			$P_{Q1N}$	$P_{Q2N}$	$P_{Q3N}$	$P_{Q4N}$	$P_{Q5N}$	$P_{Q6N}$
			(kN)	(kN)	(kN)	(kN)	(kN)	(kN)
RCF_3.3	27.7; 8.9	22.2; 7.1	63.8	84.6	84.6	63.8	-	-
			17.5	35.0	35.0	17.5	-	-
			51.1	67.7	67.7	51.1	-	-
			14.0	28.0	28.0	14.0	-	-
RCF_10.4	34.7; 7.9 (L <sub>1</sub> &L <sub>4</sub> ) 40.1; 10.6 (L <sub>2</sub> &L <sub>3</sub> )	27.8; 6.3 (L <sub>1</sub> &L <sub>4</sub> ) 32.1; 8.5 (L <sub>2</sub> &L <sub>3</sub> )	139.5	188.8	192.4	188.8	139.5	-
			23.3	48.3	50.1	48.3	23.3	-
			111.6	151.0	154.0	151.0	111.6	-
			18.6	38.6	40.1	38.6	18.6	-
RCF_7.5	30.0; 5.8 (L <sub>1</sub> ) 34.3; 7.9 (L <sub>2</sub> &L <sub>3</sub> ) 36.1; 8.8 (L <sub>4</sub> ) 38.3; 9.9 (L <sub>5</sub> )	24.0; 4.6 (L <sub>1</sub> ) 27.4; 6.3 (L <sub>2</sub> &L <sub>3</sub> ) 28.9; 7.0 (L <sub>4</sub> ) 30.6; 7.9 (L <sub>5</sub> )	109.1	147.8	163.3	155.9	148.7	100.3
			15.2	36.7	43.0	40.0	37.1	11.3
			87.3	118.2	130.6	124.7	118.9	80.2
			12.2	29.4	34.4	32.0	29.9	9.0

Table 4 Major seismological parameters of ground motion records

Record Name	Earthquake Name	Recording Station	$M_w$	$R_{JB}$ (km)	$V_{S30}$ (m/s)	PGA (g)	PGV (cm/s)	PGD (cm)
TRINIDAD.B_B-RDL270	Trinidad, 1980	Rio Dell Overpass-FF	7.20	76.06	311.75	0.151	8.88	3.63
SUPER.B_B-POE360	Superstition Hills-02, 1987	Poe Road	6.54	11.16	316.64	0.286	29.02	11.56
LANDERS_YER360	Landers, 1992	Yermo Fire Station	7.28	23.62	353.63	0.152	29.60	24.83
KOBE_KAK000	Kobe, 1995	Kakogawa	6.90	22.50	312.00	0.240	20.80	6.39
KOBE_SHI000	Kobe, 1995	Shin-Osaka	6.90	19.40	256.00	0.225	31.33	8.38
KOCAELI_DZC180	Kocaeli, Turkey, 1999	Duzce	7.51	13.60	281.86	0.312	58.85	44.05
SIERRA.MEX_GEO090	El Mayor-Cucapah, 2010	Cerro Prieto Geothermal	7.20	8.88	242.05	0.288	49.54	40.31

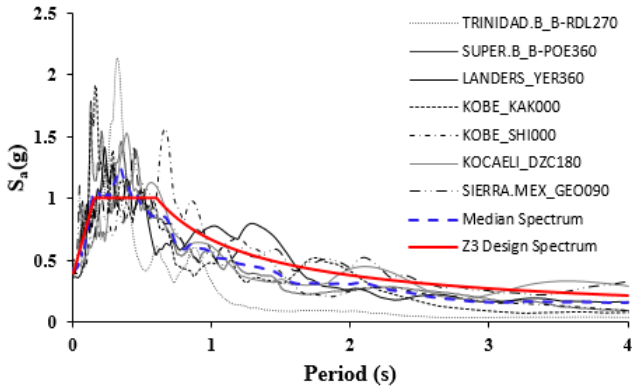


Fig. 9 Scaled spectra, median spectrum and design spectrum of TSDC

are provided. Fig. 9 shows individual linear-elastic acceleration response spectra of scaled accelerograms, their median response spectrum and the elastic design acceleration spectrum of TSDC for site class Z3, all developed for a damping ratio of 5%. Response spectra are constructed by using SeismoSpect software (SeismoSpect 2016).

## 8.2 Energy-based base shears and comparison with NLTH results

Calculation of plastic energy modification factor ( $\eta_p$ ) and input energy modification factor ( $\lambda$ ) makes essential the estimation of the ductility ratio ( $\mu$ ) and the cumulative ductility ratio ( $\eta$ ), which are both calculated from pushover

analysis. Thereby, two-dimensional nonlinear mathematical model of each frame is created in SAP2000. Initial effective stiffness values of RC components are reduced according to TSDC in order to account for cracking during the inelastic response of frames. Some fundamental dynamic parameters determined from eigenvalue analysis of frames and the input energy of the equivalent  $n$ th mode SDOF system are listed in Table 5, where  $T_n$  is the natural period of the  $n$ th mode,  $L_n = \phi_n^T \cdot M \cdot 1$ ,  $\alpha_n$  is the effective modal mass participating ratio of the  $n$ th mode and  $m_{eff,n}$  is the effective modal mass of the  $n$ th mode, respectively.

Beams and columns are modeled as nonlinear frame elements by assigning plastic hinges at both ends of these elements. An invariant lateral load pattern corresponding to the first-mode shape is used in the pushover analysis. Pushover curve of each frame is idealized as a bilinear force-deformation curve according to FEMA-356 (2000). The yield displacement and the yield base shear are taken as the coordinates of the intersection point of idealized curves while the ultimate displacement is determined as the state at which frame reaches its deformation capacity. Substituting the parameters obtained from pushover analysis together with other available parameters in Eqs. (33)-(40) and solving the derived equations within the study, energy-based yield base shears ( $V_y$ ) are obtained. The energy-based yield base shears are modified by overstrength reduction factor in order to make them useful in seismic design. The resultant design base shear ( $V_d$ ) of frames is summarized in Table 6.

As can be concluded from the table, the derived energy-based design base shears highly depend on hysteretic

Table 5 Equivalent SDOF system properties of frames

Mode no ( $n$ )	RCF_3.3			RCF_10.4			RCF_7.5		
	1	2	3	1	2	3	1	2	3
$T_n$ (s)	0.71	0.22	0.12	1.49	0.48	0.26	1.01	0.32	0.18
$L_n$ (tons)	153.379	-62.645	59.777	984.152	-359.061	228.055	741.838	-268.683	172.371
$M_n$ (tons)	120.504	171.650	656.094	750.204	728.872	735.390	570.531	577.090	637.338
$\Gamma_n$	1.273	-0.365	0.091	1.312	-0.493	0.310	1.300	-0.466	0.270
$\alpha_n$ (%)	87.24	10.22	2.43	77.85	10.65	4.26	81.37	10.54	3.93
$m_{eff,n}$ (tons)	195.23	22.87	5.44	1290.92	176.60	70.64	964.43	124.92	46.58
$E_{I,n}$ (kNm)	56.56	10.13	8.92	473.58	204.68	60.59	308.06	72.03	25.17

Table 6 Energy-based design base shears (kN) of frames

Frame	$\zeta_H$	Eq. (20)	Eq. (21)	Eq. (22)	Eq. (23)
RCF_3.3		457.12	327.49	546.51	392.04
RCF_10.4	Eq. (15)	1446.85	1079.38	1842.55	1343.25
RCF_7.5		1119.46	972.79	1553.32	1200.45
RCF_3.3		424.59	301.43	510.28	362.58
RCF_10.4	Eq. (16)	1344.00	995.66	1718.48	1246.35
RCF_7.5		1140.36	991.20	1581.19	1222.70
RCF_3.3		458.32	328.46	547.84	393.13
RCF_10.4	Eq. (17)	830.71	604.91	1080.83	766.73
RCF_7.5		609.46	527.02	857.69	982.96
RCF_3.3		398.50	280.92	480.91	339.15
RCF_10.4	Eq. (18)	1503.60	1121.30	1910.45	1396.84
RCF_7.5		804.97	697.17	1127.62	864.77

damping ( $\zeta_H$ ) and input energy modification factor ( $\lambda$ ). Different approaches on estimation of  $\zeta_H$  and  $\lambda$ , yield different design base shear values. The minimum base shears are obtained calculating  $\lambda$  from Eq. (21), while considering  $\lambda$  of Eq. (22) gives the maximum base shears for all different approaches used in estimation of  $\zeta_H$ . For the same  $\lambda$  values,  $\zeta_H$  calculated from Eq. (15) and (17) yields almost the same design base shears of RCF\_3.3, while similar design base shears are obtained using  $\zeta_H$  calculated from Eq. (15) and (18) for RCF\_10.4 and  $\zeta_H$  calculated from Eq. (15) and (16) for RCF\_7.5. For the same values of  $\zeta_H$ , there is no any  $\lambda$  value yielding similar design base shear in frames.

The scattered results of energy-based design base shears are compared with those obtained from NLTH analysis. NLTH analyses of frames are performed by using the time histories of the scaled ground motions compatible with the elastic design acceleration spectrum of TSDC (2007). Since seven recorded accelerograms are selected, totally 21 NLTH analyses are performed considering the nonlinear structural models created in SAP2000 environment and the average value of the maximum base shears is taken into consideration. Modal damping ratio is taken as 5% and Rayleigh damping model, which assumes that the damping is proportional to a linear combination of the stiffness and mass (Chopra 1995), is used in dynamic analyses. The mean base shears and the mean plus/minus the standard deviation of the mean base shears of NLTH analysis are shown together with energy-based story shears of frames in Figs. 10-12, where energy-based base shears are distributed to each story level according to the procedure given in TSDC (2007).

The mean design base shears and the mean plus/minus the standard deviation of the mean design base shears obtained from NLTH analysis generally range between energy-based design base shears calculated considering different approximations of hysteretic damping and input energy modification factor. The mean shear forces of NLTH analysis are bigger than energy-based ones in the last story of RCF\_3.3, while they vary between energy-based shear forces in lower stories. Similarly, bigger story shear forces

are obtained from NLTH analysis for the last three stories of RCF\_10.4 and RCF\_7.5 when compared to energy-based story shears. Energy-based design base shear forces  $V_{d,energy}=392.04$  kN ( $\zeta_H$  from Eq. (15) and  $\lambda$  from Eq. (23)) and  $V_{d,energy}=393.13$  kN ( $\zeta_H$  from Eq. (17) and  $\lambda$  from Eq. (23)) are found to be very close to the mean base shear of NLTH analysis  $V_{d,NLTH}=383.27$  kN for RCF\_3.3. Three energy-based design base shears,  $V_{d,energy}=1343.25$  kN ( $\zeta_H$  from Eq. (15) and  $\lambda$  from Eq. (23)),  $V_{d,energy}=1344.00$  kN ( $\zeta_H$  from Eq. (16) and  $\lambda$  from Eq. (20)) and  $V_{d,energy}=1396.84$  kN ( $\zeta_H$  from Eq. (18) and  $\lambda$  from Eq. (23)), are in reasonable agreement with the mean base shear obtained from NLTH

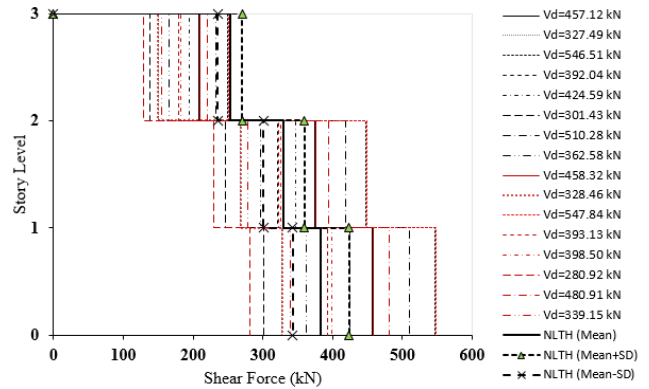


Fig. 10 Energy-based story shears and NLTH results of RCF\_3.3

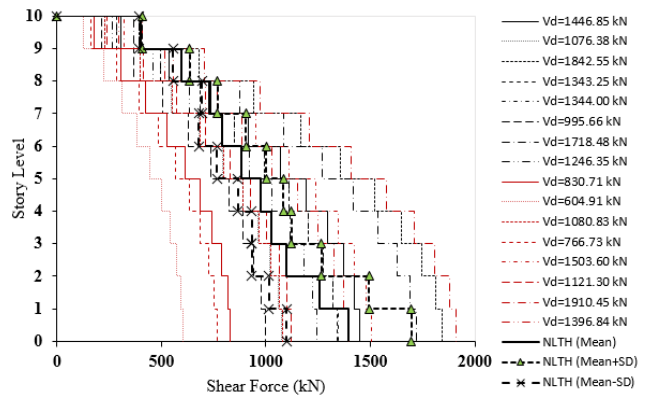


Fig. 11 Energy-based story shears and NLTH results of RCF\_10.4

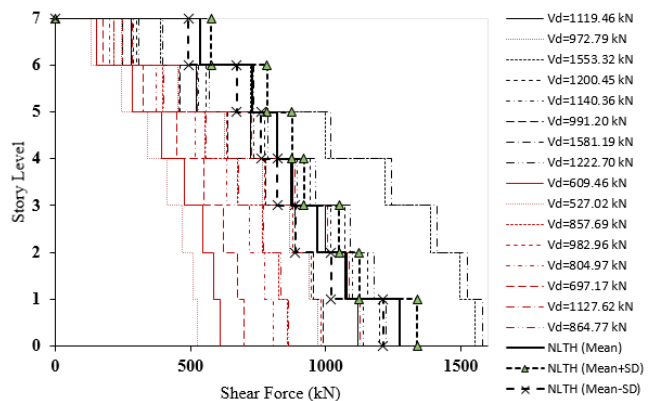


Fig. 12 Energy-based story shears and NLTH results of RCF\_7.5

analysis as  $V_{d,NLTH}=1396.79$  kN for RCF\_10.4. And, two energy-based design base shears of RCF\_7.5,  $V_{d,energy}=1200.45$  kN ( $\zeta_H$  from Eq. (15) and  $\lambda$  from Eq. (23)) and  $V_{d,energy}=1222.70$  kN ( $\zeta_H$  from Eq. (16) and  $\lambda$  from Eq. (23)) are the closest values to  $V_{d,NLTH}=1275.49$  kN, which is obtained from NLTH analysis. Generally, considering  $\zeta_H$  of Eq. (17) yields smaller design base shears in RCF\_10.4 and RCF\_7.5, when compared to results of NLTH analysis.

## 9. Conclusions

Design base shear forces based on pre-selected failure mechanism and target story drift ratio are derived for multistory RC frame structures. The modified relative energy equation, where the earthquake input energy is modified with a factor depending on damping ratio and ductility, and the plastic energy is decreased with a factor to consider the reduced hysteretic behavior of RC members, is obtained. The plastic energy obtained from energy balance is equated to external work done by the equivalent inertia forces considering and solving the derived quadratic equations, which include combinations of different energy modification factors, base shears are calculated. Relative input energy of MDOF system is approximated by summation of the energies of the first three vibration modes. NLTH analysis using seven recorded accelerograms are performed and energy-based design base shears are compared with the results of dynamic analyses.

Material nonlinearity, hysteretic properties of structural components and hysteretic damping are taken into account in a simple manner in the derived energy-based base shears, while code specific seismic design base shear forces are generally based on elastic vibration conditions. Additionally, earthquake effect is considered as energy input to the structure and type of failure mechanism and the contribution of higher modes are included in the energy-based base shears.

Scattered energy-based design base shear forces are obtained depending on the equation of hysteretic damping and input energy modification factor. It is found that, both modification factors have an important impact on consistency of energy-based design base shears. The combination of the lowest damping value and the highest input energy modification factor always results in the energy-based base shear force. Hysteretic damping formula of Priestley (2003) gives higher damping values which in turn generally results in smaller base shear forces. Since input energy modification factor directly controls the earthquake input energy to the system, it has predominant influence on energy-based base shears. The input energy modification factor of Kuwamura and Galambos (1989) gives the lowest values which in turn results in the smallest base shear forces. The highest values of input energy modification factors are obtained using the formula proposed by Fajfar and Vidic (1994) and regardless of hysteretic damping or plastic energy modification factor, the biggest base shears are obtained when the energy input modification factor proposed by Fajfar and Vidic (1994) is considered. For the same formulations of input energy

modification factor, the energy-based base shears considering hysteretic damping estimation of Gulkan and Sozen (1974) always have reasonable agreement with another base shear force.

Some of the energy-based base shears are in reasonable agreement with the mean base shear obtained from NLTH analysis. Generally, mean shear forces of NLTH analysis are bigger than energy-based ones in upper stories, while they vary between the scattered energy-based shear forces in lower stories. Since hysteretic damping formulation of Gulkan and Sozen (1974) and input energy modification factor proposed by Benavent-Climent *et al.* (2002) are common in energy-based design base shears found to be close to the mean base shear of NLTH analysis, the use of these two modification factors in derivation of energy-based base shears may be proposed.

The calculations in the study are totally based on a pre-specified global failure mechanism and energy-based design base shear forces for RC frames are derived under this condition. The selection of a different failure mechanism will probably change the energy-based base shear force equations. Further research is required to find out what will happen when this methodology is applied to a structure not exhibiting global failure mechanism.

## References

- Akbas, B. and Shen, J. (2003), "Earthquake resistant design and energy concepts", *Tech. J. Turkish Chamber Civ. Engineers*, **14**(2), 2877-2901.
- Akiyama, H. (1985), *Earthquake-Resistant Limit-State Design for Buildings*, The University of Tokyo Press, Japan.
- Bai, J. and Ou, J. (2012), "Plastic limit-state design of frame structures based on the strong-column weak-beam failure mechanism", *Proceedings of the 15th World Conference on Earthquake Engineering*, Lisboa, Portugal, September.
- Bayat, M.R., Goel, S.C. and Chao, S.H. (2008), "Further refinement of performance-based plastic design of structures for earthquake resistance", *14th World Conference on Earthquake Engineering*, Beijing, China, October.
- Benavent-Climent, A., Pujades, L.G. and Lopez-Almansa, F. (2002), "Design energy input spectra for moderate seismicity regions", *Earthq. Eng. Struct. D.*, **31**(5), 1151-1172.
- Benavent-Climent, A., Lopez-Almansa, F. and Bravo-Gonzales, D.A. (2010), "Design energy input spectra for moderate-to-high seismicity regions based on Colombian earthquakes", *Soil Dyn. Earthq. Eng.*, **30**(11), 1129-1148.
- Blandon, C.A. (2004), "Equivalent viscous damping equations for direct displacement based design", M.Sc. Dissertation, Rose School, Pavia, Italy.
- Calvi, G.M., Priestley, M.J.N. and Kowalsky, M.J. (2008), "Displacement-based seismic design of structures", *3<sup>rd</sup> National Conference on Earthquake Engineering and Engineering Seismology*, Athens, Greece, November.
- Chao, S.H. and Goel, S.C. (2005), "Performance-based seismic design of ebf using target drift and yield mechanism as performance criteria", Research Report MI 48109-2125; The University of Michigan, Ann Arbor.
- Chopra, A.K. (1995), *Dynamics of Structures, Theory and Applications to Earthquake Engineering*, Prentice Hall, Upper Saddle River, NJ.
- Chou, C.C. and Uang, C.M. (2003), "A procedure for evaluating seismic energy demand of framed structures", *Earthq. Eng.*

- Struct. D.*, **32**(2), 229-244.
- Dogru, S., Aksar, B., Akbas, B., Shen, J. and Doran, B. (2015), "Seismic energy response of two-story X-braced frames", *3rd Turkish Conference on Earthquake Engineering and Seismology*, Izmir, Turkey, October.
- Dwairi, H.M. (2004), "Equivalent damping in support of direct displacement-based design with applications to multi-span bridges", Ph.D. Dissertation, North Carolina State University, Raleigh, North Carolina.
- Dwairi, H.M., Kowalsky, M.J. and Nau, J.M. (2007), "Equivalent damping in support of direct displacement-based design", *J. Earthq. Eng.*, **11**(4), 512-530.
- Ezz, A.A.E. (2008), "Deformation and strength based assessment of seismic failure mechanisms for existing RC frame buildings", M.Sc. Dissertation, European School for Advanced Studies in Reduction of Seismic Risk, Rose School, Pavia, Italy.
- Fajfar, P. and Vidic, T. (1994), "Consistent inelastic design spectra: hysteretic and input energy", *Earthq. Eng. Struct. D.*, **23**(5), 523-537.
- FEMA P440A (2009), Effects of strength and stiffness degradation on seismic response, Applied Technology Council; Redwood City, California.
- FEMA-356 (2000), Prestandard and commentary for the seismic rehabilitation of buildings, Federal Emergency Management Agency; Washington DC.
- Greco, R. (2014), "Energetic considerations on the effects of inelastic stiffness on nonlinear seismic response", *Recent Advances in Applied Mathematics, Modelling and Simulation; Proceedings of the 8th International Conference on Applied Mathematics, Simulation, Modelling (ASM'14)*, Mastorakis, N.E., Demiralp, M., Mukhopadhyay, N., Mainardi, F. (editors), 270-285, WSEAS Press, Sofia.
- Gulkan, P. and Sozen M.A. (1974), "Inelastic responses of reinforced concrete structures to earthquakes motions", *ACI Journal, Proceedings*, **71**(12), 604-610.
- Housner, G.W. (1956), "Limit design of structures to resist earthquakes", *Proceedings of the First World Conference on Earthquake Engineering*, Berkeley, California, USA, June.
- Jacobsen L.S. (1930), "Steady forced vibrations as influenced by damping", *ASME Transactione*, **52**(1), 169-181.
- Kalkan, E. and Kunnath, S.K. (2007), "Effective cyclic energy as a measure of seismic demand", *J. Earthq. Eng.*, **11**(5), 725-751.
- Kappos, A.J., Saiidi, M.S., Aydinoglu, M.N. and Isakovic, T. (editors) (2012), *Seismic Design and Assessment of Bridges: Inelastic Methods of Analysis and Case Studies*, Springer, NY.
- Kazantzi, A.K. and Vamvatsikos, D. (2012), "A study on the correlation between dissipated hysteretic energy and seismic performance", *15th World Conference on Earthquake Engineering*, Lisboa, Portugal, September.
- Khan, E., Kowlasky, M.J. and Nau, J.M. (2016), "Equivalent viscous damping model for short-period reinforced concrete bridges", *J. Bridge Eng.*, **21**(2), 04015047.
- Kim, H.J. (2012), "Seismic response of flag-shaped hysteretic SDOF systems with seismic fuses", *Int. J. Steel Struct.*, **12**(4), 523-535.
- Kowalsky, M.J. (1994), "Displacement based design: A methodology for seismic design applied to RC bridge columns", M.Sc. Dissertation, University of California, San Diego.
- Kuwamura, H. and Galambos, T. (1989), "Earthquake load for structural reliability", *J. Struct. Eng.*, **115**(6), 1446-1462.
- Leelataviwat, S., Goel, S.C. and Stojadinovic, B. (2002), "Energy-based seismic design of structures using yield mechanism and target drift", *J. Struct. Eng.*, **128**(8), 1046-1054.
- Leelataviwat, S., Seawon, W. and Goel, S.C. (2008), "An energy based method for seismic evaluation of structures", *14th World Conference on Earthquake Engineering*, Beijing, China, October.
- Leelataviwat, S., Saewon, W. and Goel, S.C. (2009), "Application of energy balance concept in seismic evaluation of structures", *J. Struct. Eng.*, **135**(2), 113-121.
- Liao, W.C. (2010), "Performance-based plastic design of earthquake resistant reinforced concrete moment frames", Ph.D. Dissertation, The University of Michigan, Ann Arbor, USA.
- Lieping, Y. and Zhe, Q. (2009), "Failure mechanism and its control of building structures under earthquakes based on structural system concept", *J. Earthq. Tsunami*, **3**(4), 249-259.
- Lopez-Almansa, F., Yazgan, A.U. and Benavent-Climent, A. (2013), "Design energy input spectra for high seismicity regions based on Turkish registers", *Bull. Earthq. Eng.*, **11**(4), 885-912.
- Massumi, A. and Monavari, B. (2013), "Energy based procedure to obtain target displacement of reinforced concrete structures", *Struct. Eng. Mech.*, **48**(5), 681-695.
- Mergos, P.E. and Beyler, K. (2014), "Loading protocols for European regions of low to moderate seismicity", *Bull. Earthq. Eng.*, **12**(6), 2507-2530.
- Muljati, I., Asisi, F. and Willyanto, K. (2015), "Performance of force based design versus direct displacement based design in predicting seismic demands of regular concrete special moment resisting frames", *Procedia Eng.*, **125**, 1050-1056.
- Pampamin, S., Christopoulos, C. and Priestley, M.J.N. (2002), *Residual Deformations in the Performance-Based Seismic Assessment of Frame Structures*, IUSS Press, Pavia, Italy.
- Paolacci, F. (2013), "An energy-based design for seismic resistant structures with viscoelastic dampers", *Earthq. Struct.*, **4**(2), 219-239.
- Priestley, M.J.N. (1996), "Displacement-based seismic assessment of existing reinforced concrete buildings", *Bull. NZ. Nat. Soc. Earthq. Eng.*, **29**(4), 256-272.
- Priestley, M.J.N. (2003), "Myths and fallacies in earthquake engineering, revisited", The Ninth Mallet Milne Lecture; European School for Advanced Studies in Reduction of Seismic Risk, Rose School, Pavia, Italy.
- Priestley, M.J.N., Calvi, G.M. and Kowalsky, M.J. (2007), *Displacement-Based Seismic Design of Structures*, IUSS Press, Pavia, Italy.
- PEER (2016), Pacific Earthquake Engineering Research Center Strong Ground Motion Database, <http://ngawest2.berkeley.edu/>
- Rodrigues, H., Varum, H., Arede, A. and Costa, A. (2012), "A comparative analysis of energy dissipation and equivalent viscous damping of RC columns subjected to uniaxial and biaxial loading", *Eng. Struct.*, **35**, 149-164.
- SAP2000 Ultimate (2016), Integrated Solution for Structural Analysis and Design, Computers and Structures Inc. (CSI), Berkeley, California, USA.
- SeismoSpect (2016), Seismosoft, Earthquake Engineering Software Solutions, Pavia, Italy.
- TSDC (2007), Turkish seismic design code, Ministry of Public Works and Settlement; Ankara, Turkey.
- TS500 (2000), Requirements for design and construction of reinforced concrete structures, Turkish Standards Institution; Ankara, Turkey.
- Uang, C.M. and Bertero, V.V. (1990), "Evaluation of seismic energy in structures", *Earthq. Eng. Struct. D.*, **19**(1), 77-90.
- Yazgan, U. (2010), "The use of post-earthquake residual displacements as a performance indicator in seismic assessment", Ph.D. Dissertation, ETH Zurich, Zurich.
- Ye, L.P., Lu, X.Z., Ma, Q.L., Cheng, G.Y., Song, S.Y., Miao, Z.W. and Pan, P. (2008), "Study on the influence of post-yielding stiffness to the seismic response of building structures", *14th World Conference on Earthquake Engineering*, Beijing, China, October.